ISSN 0036-0236, Russian Journal of Inorganic Chemistry, 2008, Vol. 53, No. 9, pp. 1353–1358. © Pleiades Publishing, Ltd., 2008.
Original Russian Text © P.S. Berdonosov, V.A. Dolgikh, 2008, published in Zhurnal Neorganicheskoi Khimii, 2008, Vol. 53, No. 9, pp. 1451–1456.

SYNTHESIS AND PROPERTIES OF INORGANIC COMPUNDS

Copper Lanthanide Selenite Oxohalides with Francisite Structure: Synthesis and Structural Characteristics

P. S. Berdonosov and V. A. Dolgikh

Moscow State University, Moscow, 119992 Russia

Received July 12, 2007

Abstract—The reaction of lanthanide oxohalides with CuO and SeO_2 gave the products $Cu_3Ln(SeO_3)_2O_2X$ (Ln = lanthanide, X = Cl, Br). The oxochlorides are formed with all lanthanides, while oxobromides are formed only for Ln = La–Gd. The structures of the $Cu_3Ln(SeO_3)_2O_2Cl$ phases for Ln = Nd (**I**) and Y (**II**) were determined by the Rietveld method. It was found that $Cu_3Ln(SeO_3)_2O_2X$ has the structure of francisite (orthorhombic system, space group *Pmmn*), which does not change substantially upon the variation of the Ln^{3+} radius. No similar compounds with tellurium(IV) were found.

DOI: 10.1134/S0036023608090027

Inorganic compounds containing simultaneously a complex anion and an elemental anion have attracted in recent years keen attention of researchers due to expected unusual structures of such phases and the presence of important applied properties. Thus a large number of structures with low dimensionality and with open frameworks containing channels or cavities is expected for the selenite halide class [1]. In addition, the presence of an acentric SeO_3 group in the crystal increases the probability of formation of a noncentrosymmetric structure [2], which is a necessary condition for the appearance of nonlinear-optical and piezo- and pyroelectric properties.

Meanwhile, selenite halides are represented in most cases by only parent compounds of the potential families. These include the family of phases with a francisite-type structure. The prototype of this structural type, francisite $Cu_3Bi(SeO_3)_2O_2Cl$ (**III**) has been described rather long ago [3]. Subsequently, both its synthetic analogue and isostructural compounds with other halogens, $Cu_3Bi(SeO_3)_2O_2X$ (X = Cl, Br, I), have been obtained [4]. The possibility of replacement of selenium by tellurium ($Cu_3Bi(TeO_3)_2O_2Cl$ [5]) and bismuth by lanthanide ($Cu_3Er(SeO_3)_2O_2Cl$ (**IV**) [6]) with retention of the key features of the francisite structure was demonstrated.

This structure is based on an open framework formed by highly distorted [BiO_8] cubes, [CuO_4] squares, and [SeO_3] pyramids; the voids of this framework accommodate chloride anions separated from the bismuth atoms by distances of more than 4 Å and from copper atoms by 3.07 Å.

The variation of the types of halogens in bismuth-containing phases of this family results in a regular increase of unit cell parameters and elongation of the corresponding bonds [4].

The replacement of selenium by the larger tellurium atom induces a substantial transformation of the prototype structure. In $Cu_3Bi(TeO_3)_2O_2Cl$ (**V**) [5], the oxygen atoms are displaced from the highly symmetrical crystallographic positions, which gives rise to an additional position, and the distance from one of the two crystallographically independent copper atoms (Cu(2)) to the chlorine atom is markedly shortened, resulting in transformation of Cu(2) coordination into square-pyramidal [$Cu(2)O_4Cl$]. Finally, the unit cell parameter *c* in telluride oxochloride is doubled and the space group is changed compared to francisite (*Pcmn* for **V** and *Pmmn* for francisite **III**).

At the same type, the structure of erbium-containing phase **IV** [6] has no key differences from the parent francisite structure **III**, which prompts the idea that a broad series of analogous phases with other lanthanides could exist.

However, apart from **IV**, we found in the literature only a mention of the preparation of analogous compounds with La and Nd [6] but no structural data were reported. On the other hand, it is known that lanthanide compounds with the same stoichiometry may have different structures with different lanthanide cations or exist only for a particular set of lanthanides [7–9].

In this paper, we report the results of a search for Cu–Ln telluride oxochlorite, the synthesis conditions, and X-ray diffraction characteristics for the $Cu_3Ln(SeO_3)_2O_2X$ phases (X = Cl, Br; Ln = La, Nd, Sm, Eu, Gd, Dy, Ho, Er, Yb).

Table 1. Unit cell parameters and volumes for $Cu_3Ln(SeO_3)_2O_2X$ (X = Cl, Br), space group *Pmmn*

X = Cl	*a*, Å	*b*, Å	*c*, Å	*V*, Å^3
La	6.398(1)	9.725(1)	7.154(1)	445.05(8)
Nd	6.362(1)	9.606(1)	7.074(1)	432.36(8)
Eu	6.333(3)	9.497(4)	7.016(3)	422.00(2)
Gd	6.3220(6)	9.501(1)	7.0202(8)	421.66(6)
Dy	6.313(1)	9.465(2)	6.987(2)	417.5(1)
Ho	6.2999(6)	9.440(1)	6.9723(8)	414.65(5)
Er	6.2921(7)	9.4257(9)	6.9632(9)	412.97(6)
Yb	6.2803(8)	9.381(1)	6.927(2)	408.1(1)
Y	6.2938(9)	9.438(1)	6.970(1)	414.33(8)
X = Br				
La	6.405(2)	9.888(4)	7.142(3)	452.4(2)
Nd	6.382(2)	9.698(3)	7.091(2)	438.9(2)
Sm	6.348(1)	9.581(2)	7.079(2)	430.6(1)
Gd	6.337(1)	9.5515(8)	7.0540(9)	426.96(7)

EXPERIMENTAL

Synthesis and characteristics of samples. Lanthanide oxohalides LnOX (Ln = La, Nd, Sm, Eu, Gd, Dy, Ho, Er, Yb, and Y; X = Cl, Br), copper oxide (special purity grade 9-2), and selenium or tellurium dioxide served as the starting compounds.

The oxohalides LnOX were prepared by pyrolysis of lanthanide trihalide hydrates in an air flow at 550–400°C depending on the particular halogen and lanthanide. Selenium dioxide was obtained from selenous acid (98%), which was dehydrated under dynamic vacuum at moderate temperatures. The product was then sublimed in a flow of a mixture of dry air and NO_2 prepared by thermal decomposition of $Pb(NO_3)_2$ (analytical grade). All weighing and preparatory operations with SeO_2 were carried out in a dry box purged with argon. Tellurium dioxide was prepared by a reported procedure [10]: tellurium was dissolved in aqua regia at 80°C and crystalline TeO_2 was precipitated by aqueous ammonia.

The single-phase nature of the products was confirmed by powder X-ray diffraction. The measurements were carried out in an FR-552 Guinier type camera (Enraf-Nonius) or on a Stadi-p Stoe diffractometer ($CuK_{\alpha 1}$ radiation). The conclusion about the phase composition of the product was based on PDF-2 database [11].

The above-described precursors were used to prepare stoichiometric mixtures according to the equation

$$3CuO + LnOX + 2AO_2 \longrightarrow Cu_3Ln(AO_3)_2O_2X$$
(A = Se, Te; X = Cl, Br).

The components were weighed on a Sartorius Gem^{plus} balance (accuracy 0.0002 g). The overall sample weight did not exceed 0.7 g. The mixtures were thoroughly ground in an agate mortar and transferred into quartz ampoules, which were sealed off under vacuum (~10^{-2} mm Hg) and placed into annealing furnaces with controlled heating. The annealing mode was varied depending on the starting components. The batch containing SeO_2 was heated to 300°C over a period of 6–12 h and kept at this temperature for 12–24 h. Then the temperature was raised to 550°C during 6 h, and the batch was kept at this temperature for 7 days. Samples containing TeO_2 were heated directly to 550°C during 3 h and kept at this temperature for 7 days.

The annealing gave green-colored powdered products. A visual examination of the samples under an optical microscope showed the presence of white-colored grains in all tellurium-containing samples. All selenium chloride samples looked uniformly colored and the bromide products fell into two groups as regards the appearance: uniformly colored samples (Ln = La, Nd, Sm, Gd) and powders containing grains with different tints (Ln = Dy, Er, Yb).

Powder X-ray diffraction of tellurium derivatives confirmed that they were not single phases. No desired compounds with a francisite-type structure were found among them, lanthanide tellurites $Ln_2Te_4O_{11}$ being the major components. Other reaction products were apparently copper oxochloride derivatives, which were unstable against hydrolysis and, hence, were not detected by X-ray diffraction.

Powder X-ray diffraction of selenium chloride derivatives and bromide derivatives with Ln = La, Nd, Sm, and Gd showed the absence of the starting copper or lanthanide selenite phases. The X-ray diffraction patterns of the samples of the two indicated groups were similar for all tested lanthanides and could be fully indexed under the assumption of the type **IV** structure. The unit cell parameters are given in Table 1.

The X-ray diffraction patterns of the samples with the formal composition $Cu_3Ln(SeO_3)_2O_2Br$ for Ln = Dy, Er, Yb differed from the above-described ones. The reflections present could not be assigned to any phases known in these systems; indexing of these X-ray diffraction patterns was impossible. This fact, together with the visual examination of samples noted above, indicate most likely that the products of annealing of mixtures involving late lanthanides are multiphase materials.

In order to elucidate the structural features of these phases, we refined the structures of two selenite oxochlorides by the Rietveld method. This was carried out for Nd and Y derivatives, because the radii of these

Table 2. Crystal data and X-ray diffraction experiment detail for $Cu_3Ln(SeO_3)_2O_2Cl$ (Ln = Nd(**I**), Y(**II**))

	I	II
System	Orthorhombic	Orthorhombic
Space group	*Pmmn*	*Pmmn*
Unit cell parameters		
a, Å	6.37775(10)	6.30963(5)
b, Å	9.62685(16)	9.45637(7)
c, Å	7.09341(11)	6.98355(5)
Z	2	2
2θ range, deg	10–114	10–115
The number of refined parameters	39	41
R_p	0.0273	0.0499
wR_p	0.0390	0.0726

Ln^{3+} ions differ considerably [12]; hence, this is the pair of choice for comparison.

Polycrystalline $Cu_3Ln(SeO_3)_2O_2Cl$ samples (Ln = Nd (**I**), Y (**II**)) were studied on a Stoe Stadi-p diffractometer equipped with a germanium monochromator ($CuK_{\alpha 1}$ radiation) in the 2θ range of 10°–115° with a step of 0.01°. The resulting X-ray diffraction patterns were processed by the GSAS program [13]. As the initial model, the structural data for **IV** were used [6]. The X-ray diffraction experiment details are summarized in Table 2, the atomic coordinates and thermal parameters are given in Table 3, and selected interatomic distances are in Table 4. The final Rietveld refinement profiles are shown in Fig. 1. The X-ray diffraction pattern of sample **II** showed four weak peaks from an impurity in the 2θ range of 24°–28°, which could not be assigned to any known phases. This accounts for somewhat higher *R* factors in the solution of structure **II** as compared to **I**.

RESULTS AND DISCUSSION

The desired selenite oxohalides formed in most of our experiments. The structures of phases **I** and **II** (Fig. 2) are typical of the francisite family, which seems to cover the selenite oxochlorite derivatives of all lan-

Table 3. Atomic coordinates and isotropic thermal parameters for **I** and **II**

Atom	Position	*x*	*y*	*z*	U_{iso}, Å^2
I					
Nd(1)	2*a*	0.25	0.25	0.26709(21)	0.0102(6)
Cu(1)	4*c*	0.0	0.0	0.0	0.0479(10)
Cu(2)	2*a*	0.25	0.25	0.7890(6)	0.0301(13)
Se(1)	4*e*	0.25	0.55626(20)	0.59867(27)	0.0202(7)
Cl(1)	2*b*	0.25	0.75	0.1596(8)	0.0427(23)
O(1)	4*e*	0.25	0.1097(10)	0.9864(14)	0.0328(17)
O(2)	8*g*	0.0450(9)	0.5833(6)	0.7499(11)	0.0328(17)
O(3)	4*e*	0.25	0.1250(9)	0.5760(15)	0.0328(17)
II					
Y(1)	2*a*	0.25	0.25	0.26583(18)	0.0036(4)
Cu(1)	4*c*	0.0	0.0	0.0	0.0120(4)
Cu(2)	2*a*	0.25	0.25	0.79490(29)	0.0108(6)
Se(1)	4*e*	0.25	0.55992(11)	0.59026(15)	0.00434(31)
Cl(1)	2*b*	0.25	0.75	0.1461(5)	0.0257(12)
O(1)	4*e*	0.25	0.1128(6)	0.9972(9)	0.0195(20)
O(2)	8*g*	0.0397(7)	0.5871(5)	0.7398(7)	0.0199(16)
O(3)	4*e*	0.25	0.1214(6)	0.5726(9)	0.0175(21)

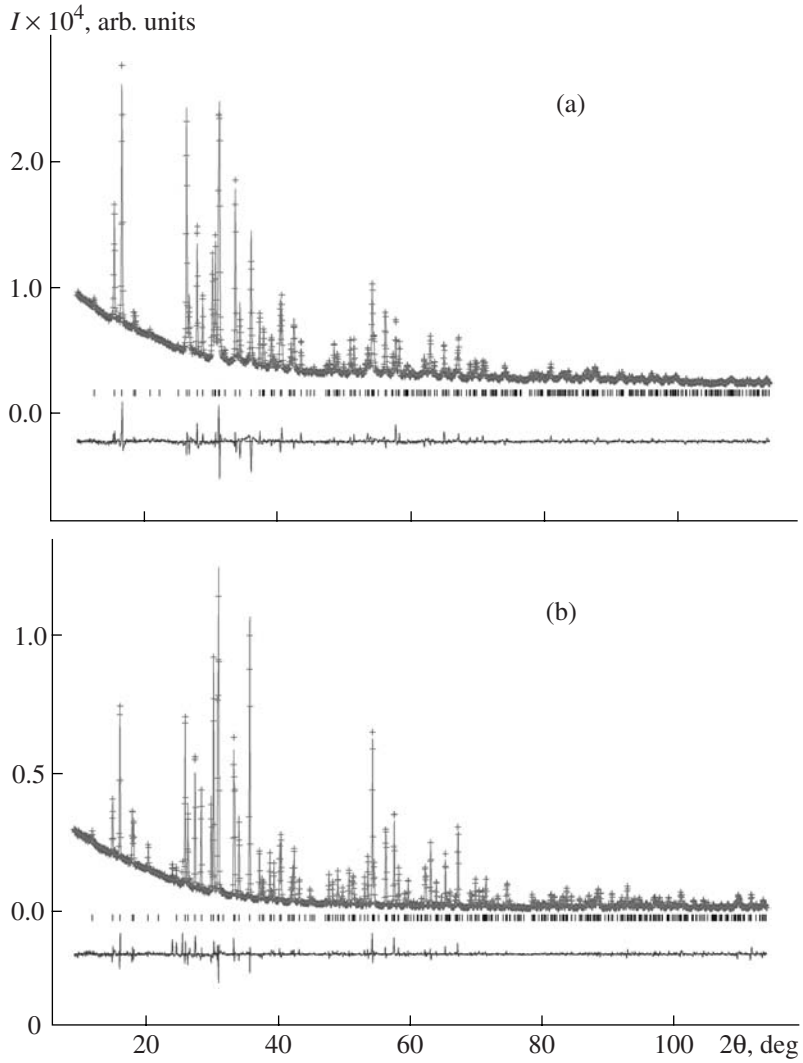

Fig. 1. Final Rietveld refinement profiles for (a) **I** and (b) **II**. The experimental profiles are shown by crosses and the calculated ones are shown by the continuous line. The strokes correspond to the theoretical positions of peaks in the X-ray diffraction patterns. Figs. 1a and 1b present also the difference curve between the calculated and theoretical profiles.

Table 4. Interatomic distances (*d*) in structures **I** and **I**

I			II		
Bond		*d*, Å	Bond		*d*, Å
Nd(1)–O(1)	×2	2.406(9)	Y(1)–O(1)	×2	2.281(6)
Nd(1)–O(2)	×4	2.476(6)	Y(1)–O(2)	×4	2.391(4)
Nd(1)–O(3)	×2	2.500(10)	Y(1)–O(3)	×2	2.464(7)
Cu(1)–Cl(1)	×2	3.101(2)	Cu(1)–Cl(1)	×2	3.020(1)
Cu(1)–O(1)	×2	1.915(5)	Cu(1)–O(1)	×2	1.904(3)
Cu(1)–O(2)	×2	1.968(8)	Cu(1)–O(2)	×2	2.011(5)
Cu(2)–O(1)	×2	1.945(10)	Cu(2)–O(1)	×2	1.918(6)
Cu(2)–O(3)	×2	1.932(9)	Cu(2)–O(3)	×2	1.972(6)
Cu(2)–Cl(1)	×2	3.210(1)	Cu(2)–Cl(1)	×2	3.182(1)
Se(1)–O(2)	×2	1.711(7)	Se(1)–O(2)	×2	1.708(4)
Se(1)–O(3)		1.753(9)	Se(1)–O(3)		1.719(6)

thanides. As in prototype **III**, in the structures of **I** and **II**, two copper atoms have square coordination by oxygen atoms. These squares share vertices and form layers perpendicular to the [001] direction; the layers are cross-linked by LnO_8 cubes to form a hollow framework.

The selenium atoms have a usual trigonal bipyramidal SeO_3 coordination completed by the lone electron pair (LEP) of Se(IV) functioning as an additional ligand. The SeO_3 pyramids share vertices with CuO_4 squares of only one layer (Fig. 2). Chloride ions not incorporated in the coordination polyhedra are arranged in the framework tunnels together with LEP.

The main specific features introduced in the structure by the lanthanide nature are related to the change in bond lengths. A comparison of the Cu(1)–O and Cu(2)–O bond for erbium [10], neodymium, and yttrium

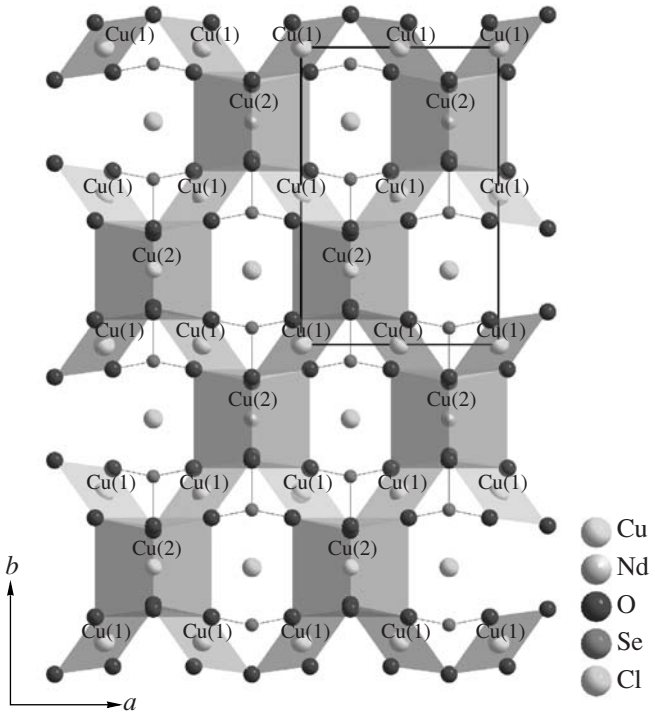

Fig. 2. Structure of $Cu_3Nd(SeO_3)_2O_2Cl$ (**I**). A unit cell is shown and Nd and Cu polyhedra are marked.

compounds shows that the bond length differences for different copper atoms $\Delta_1 = r_{(Cu(1)-O(1))} - r_{(Cu(1)-O(2))}$ and $\Delta_2 = r_{(Cu(2)-O(1))} - r_{(Cu(2)-O(3))}$ are relatively great for erbium and yttrium compounds (Δ_1 ~ 0.1 Å, Δ_2 ~ 0.06 Å), while for the compound with larger Nd^{3+} cation, Δ_1 is ~0.05 Å and Δ_2 is ~0.01 Å. Presumably, this is due to the elongation of the Ln–O bonds in the case of neodymium as compared to yttrium and erbium (Table 4) since $[CuO_4]$ squares share edges with lanthanide polyhedra $[LnO_8]$ (Fig. 2).

The higher degree of distortion of SeO_3pyramids in phase **I** compared to **II** (Table 4) may be regarded as being due to this transformation of Cu–O distances since the SeO_3 polyhedra share vertices with the $[Cu(1)O_4]$ and $[Cu(2)O_4]$ squares (Fig. 2).

In the case of selenite oxobromides, phases with a francisite-type structure end at gadolinium, which may be due to the size factor. Figure 3 shows a nearly linear dependence of the unit cell volume of lanthanide selenite oxohalides with a francisite-type structure on the Ln^{3+} ion radius (CN = 8 [12]). Presumably, the large Br^- anion cannot be accommodated in the framework channels with small Ln^{3+} cations, which may give rise to the existence of a "threshold" structure.

The absence of the desired phases among our annealing products of tellurium-containing mixtures can hardly be attributed to the size factor. This aspect requires more detailed investigation.

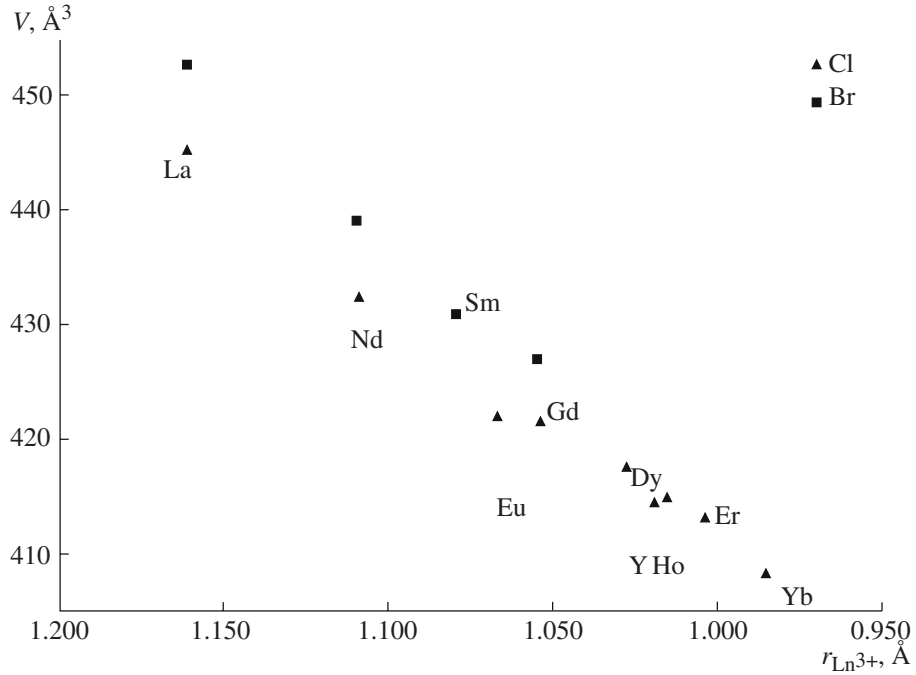

Fig. 3. Unit cell volume of the $Cu_3Ln(SeO_3)_2O_2X$ phases with the francisite-type structure vs. Ln^{3+} ion radius (CN = 8)

ACKNOWLEDGMENTS

This work was supported by the Russian Foundation for Basic Research, project nos. 06-03-32134 and 05-03-32719, and by the INTAS (YSF 05-109-4474).

REFERENCES

1. R. Becker, M. Johnsson, H. Berger, et al., Solid State Sci. **8**, 836 (2006).
2. P. S. Halasyamani and K. R. Poeppelmeier, Chem. Mater. **10**, 2753 (1998).
3. A. Pring, B. M. Gatehouse, and W. D. Birch, Am. Mineral. **75**, 1421 (1990).
4. P. Millet, B. Bastide, V. Pashchenko, et al., J. Mater. Chem. **11**, 1152 (2001).
5. R. Becker and M. Johnsson, Solid State Sci. **7**, 375 (2005).
6. R. Berrigan and B. M. Gatehouse, Acta Crystallogr., Sect. C: Struct. Sci. Commun. **52**, 496 (1996).
7. G. Brandt and R. Dieh, Mater. Res. Bull. **9** (4), 411 (1974).
8. D. G. Shabalin, P. S. Berdonosov, V. A. Dolgikh, et al., Izv. Akad. Nauk, Ser. Khim., No. 1, 93 (2003).
9. G. B. Nikiforov, P. S. Berdonosov, V. A. Dolgikh, and B. A. Popovkin, Zh. Neorg. Khim. **42** (11), 1785 (1997) [Russ. J. Inorg. Chem. **42** (11), 1632 (1997)].
10. O. I. Vorob'eva, I. A. Simanovskaya, A. S. Pashinkin, and E. A. Lavut, Izv. Vyssh. Uchebn. Zaved., Khim. Khim. Tekhnol. **9** (3), 366 (1966).
11. ICDD PDF-2 2001.
12. R. D. Shannon, Acta Crystallogr., Sect. A: Found. Crystallogr., **32**, 751 (1976).
13. A. C. Larson and R. B. Von Dreele, Los Alamos National Laboratory Report No. LA-UR-86-748,1987.